USGS
science for a changing world

Techniques of Water-Resources Investigations
of the United States Geological Survey

Chapter A4

A MODULAR FINITE-ELEMENT MODEL (MODFE) FOR AREAL AND AXISYMMETRIC GROUND-WATER FLOW PROBLEMS, PART 2: DERIVATION OF FINITE-ELEMENT EQUATIONS AND COMPARISONS WITH ANALYTICAL SOLUTIONS

By Richard L. Cooley

Book 6
Chapter A4

conjugate-gradient algorithm can sometimes yield a value of $\max_i \left|x_i^{k+1} - x_i^k\right|$ that is small even when the solution is inaccurate. Thus, another criterion that is also a rough measure of $\max_i \left|x_i - x_i^k\right|$ is employed.

The residual given by equation (270) can be written for any row i as

$$a_{i1}\left(x_1 - x_1^k\right) + a_{i2}\left(x_2 - x_2^k\right) + \ldots + a_{iN}\left(x_N - x_N^k\right) = r_i^k \qquad (286)$$

Thus, because a_{ii} is positive,

$$\frac{|a_{i1}|}{a_{ii}}\left|x_1 - x_1^k\right| + \frac{|a_{i2}|}{a_{ii}}\left|x_2 - x_2^k\right| + \ldots + \frac{|a_{iN}|}{a_{ii}}\left|x_N - x_N^k\right| \geq \frac{|r_i^k|}{a_{ii}}, \qquad (287)$$

or

$$\frac{1}{a_{ii}} \sum_{j=1}^{N} |a_{ij}| \max_i \left|x_i - x_i^k\right| \geq \frac{|r_i^k|}{a_{ii}}. \qquad (288)$$

The sum $\sum_{j=1}^{N} |a_{ij}|/a_{ii}$ is generally in the range of 1 to 2, so is assumed to be unity. Therefore, a rough measure of $\max_i \left|x_i - x_i^k\right|$ is $\left|r_i^k\right|/a_{ii}$, and the additional stopping criterion is

$$\max_i \left|r_i^k\right|/a_{ii} \leq \epsilon. \qquad (289)$$

Note that if MICCG is used to solve the nonlinear equation (234), then there will be an inner MICCG iteration loop and an outer loop on the nonlinearity. An efficient way of employing MICCG for these problems is to set the convergence criterion ϵ to be larger than normal (say, larger than ϵ_s by about an order of magnitude) to reduce the number of inner iterations taken at each outer iteration. Good accuracy is achieved by requiring close convergence of the outer iteration sequence.

COMPARISONS OF NUMERICAL RESULTS WITH ANALYTICAL SOLUTIONS

Results of simulating some simple ground-water flow problems for which analytical solutions have been presented in the literature are given here to demonstrate the accuracy of the finite-element code (MODFE). Each simulation is designed to test specific computational features that were discussed in preceding sections and to verify that MODFE can accurately represent the physical processes. To demonstrate that any consistent system of units may be used with MODFE, both English and metric systems of units are used in the example problems.

THEIS SOLUTION OF UNSTEADY RADIAL FLOW TO A PUMPED WELL

MODFE is used with axisymmetric cylindrical coordinates to compute unsteady flow to a well located in a confined nonleaky aquifer having homogeneous and isotropic hydraulic properties and an infinite areal extent.

The pumped well fully penetrates the aquifer thickness (100 feet) and its diameter (1 foot) is not significant for the simulation. The analytical solution for drawdown is given by the Theis equation (Lohman, 1972, p. 15) as

$$s = \frac{Q}{4\pi T} W(u),$$

where s is drawdown [length], Q is volumetric discharge [length^3/time], T is transmissivity [length^2/time], and W(u) is the well function

$$\int_u^\infty \frac{e^{-v}}{v} dv,$$

where $u = r^2S/4Tt$, r is radial distance from the well [length], and S is the storage coefficient [0].

Because of radial symmetry about the well bore, the problem can be simulated as an r - z plane section through the aquifer with the well located at the z axis (figure 18). The radial extent of the simulated-aquifer region is 8,000 feet, although the analytical solution was developed for an aquifer of infinite areal extent. This distance is beyond the influence of the pumped well during the simulation period so that the computed solution near the well is not affected by the boundary condition at r = 8,000 feet. Radial node spacing was expanded by a factor of $\sqrt{2}$ starting with r = 125 feet to obtain the finite-element mesh composed of 52 triangular elements and 42 nodes shown in figure 18. The initial time-element size was 3×10^{-5} days, and an expansion factor of 1.25 was used to generate subsequent elements, to yield a total of 20 time elements. Other characteristics of the problem are:

$$T = 10^5 \text{ ft}^2/\text{d},$$

$$S = 0.001,$$

$$Q = 160{,}000 \text{ ft}^3/\text{d},$$

$$h(r,z,0) = 0 \text{ ft},$$

$$h(8{,}000,z,t) = 0 \text{ ft}.$$

These characteristics and time-element sizes are the same as used by Wilson and others (1979, p. 85-88) to test their finite-element code, except that

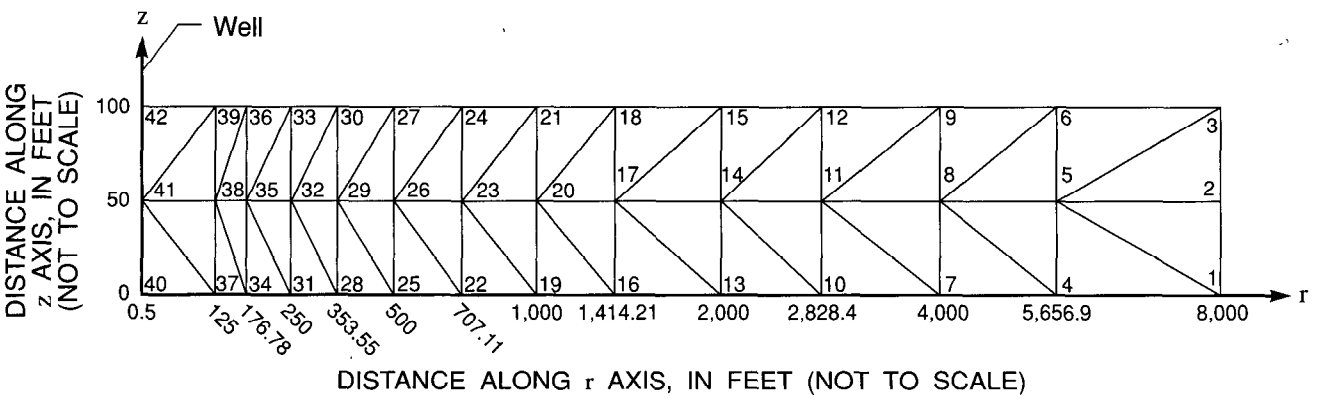

Figure 18. Finite-element mesh used to simulate unsteady-state radial flow to a pumped well.

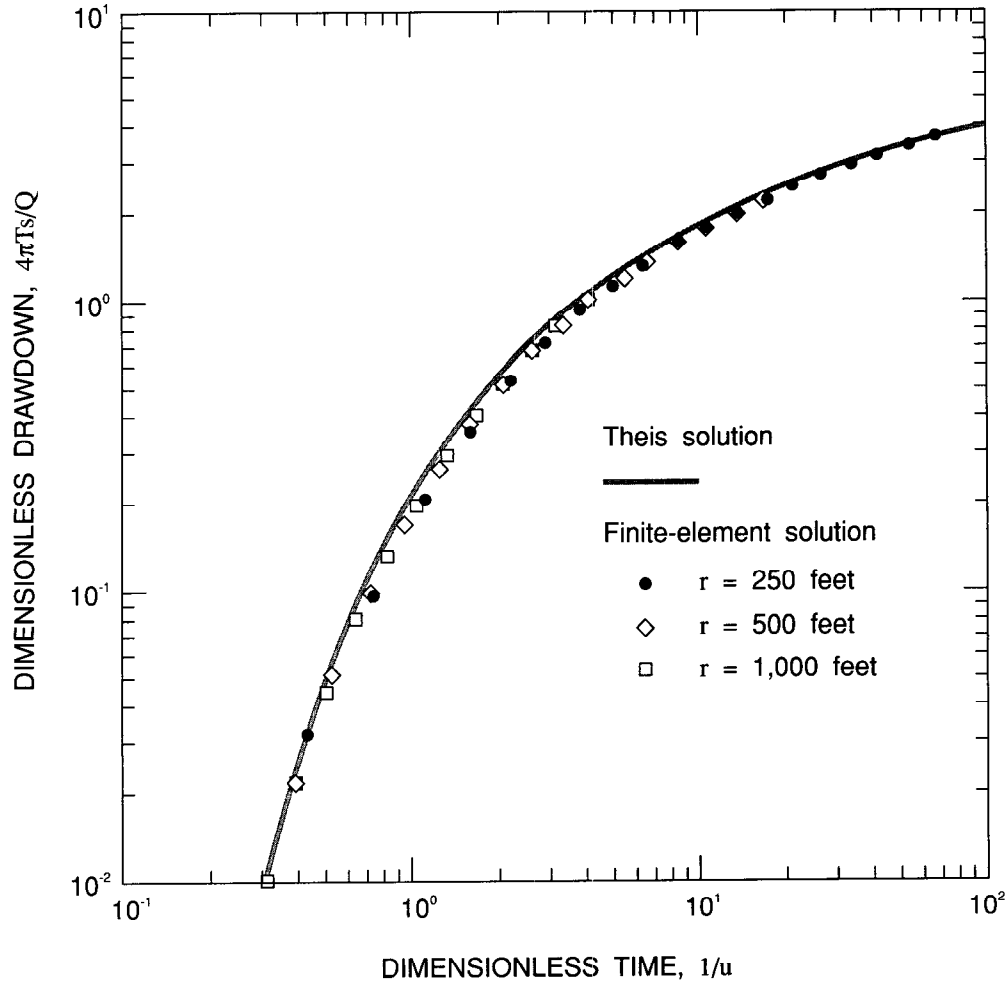

Figure 19. Theis solution (Lohman, 1972, p. 15) and finite-element results for unsteady radial flow to a pumped well.

lengths are designated as feet here rather than meters. Radial node spacing is also the same, but Wilson and others solved the problem using Cartesian coordinates.

To simulate confined flow in axisymmetric cylindrical coordinates, no-flow boundaries are placed along the aquifer top and bottom. Well discharge is simulated as a line sink at the well radius $r_w = 0.5$ feet using the specified-flow part (v_B) of the Cauchy-type boundary condition (equation (209)). Because v_B is specific discharge (volumetric discharge per unit area), it is obtained from Q as follows:

$$v_B = \frac{-Q}{2\pi r_w b} = \frac{-16{,}000}{2\pi(0.5)(100)} = -509.296 \text{ ft/d}$$

Computed values of $4\pi Ts/Q$ versus $1/u$ for the radial distances of 250, 500, and 1,000 feet are compared with the type curve of the Theis solution in figure 19. The numerical results show good agreement with the analytical solution and are nearly the same as obtained by Wilson and others (1979, p. 87) in Cartesian coordinates.

HANTUSH SOLUTION OF UNSTEADY RADIAL FLOW TO A PUMPED WELL IN A LEAKY AQUIFER

The effects of release of water stored in an elastic confining layer (transient leakage) in the vicinity of a well pumped at a constant rate in a confined, homogeneous, isotropic aquifer of infinite areal extent are contained in an analytical solution by Hantush (1960) (figure 20). The analytical solution for drawdown in this flow system is stated as (see Hantush, 1960, figure 5)

$$s = \frac{Q}{4\pi T} H(u,\beta'),$$

where $H(u,\beta')$ is an infinite integral that equals the well function $W(u)$ when $\beta' = 0$, and

$$\beta' = \frac{1}{4}\frac{r}{B}\sqrt{\frac{S'}{S}},$$

where S' is the storage coefficient ($S'_s b'$) of the confining unit and B is $\sqrt{Tb'/K'}$ [length].

The flow problem could be conceptualized with axisymmetric cylindrical coordinates, as in the first simulation. However, in order to test the transient-leakage algorithm, the flow system is represented by Cartesian coordinates. Radial symmetry is used to reduce the size of the flow domain by simulating a 22.5-degree wedge of the total flow system (see figure 21).

The finite-element mesh used in this simulation consists of 86 triangular elements and 67 nodes (figure 21) and extends 32,000 feet from the pumped well, which is placed at node 1. Node spacing increases radially

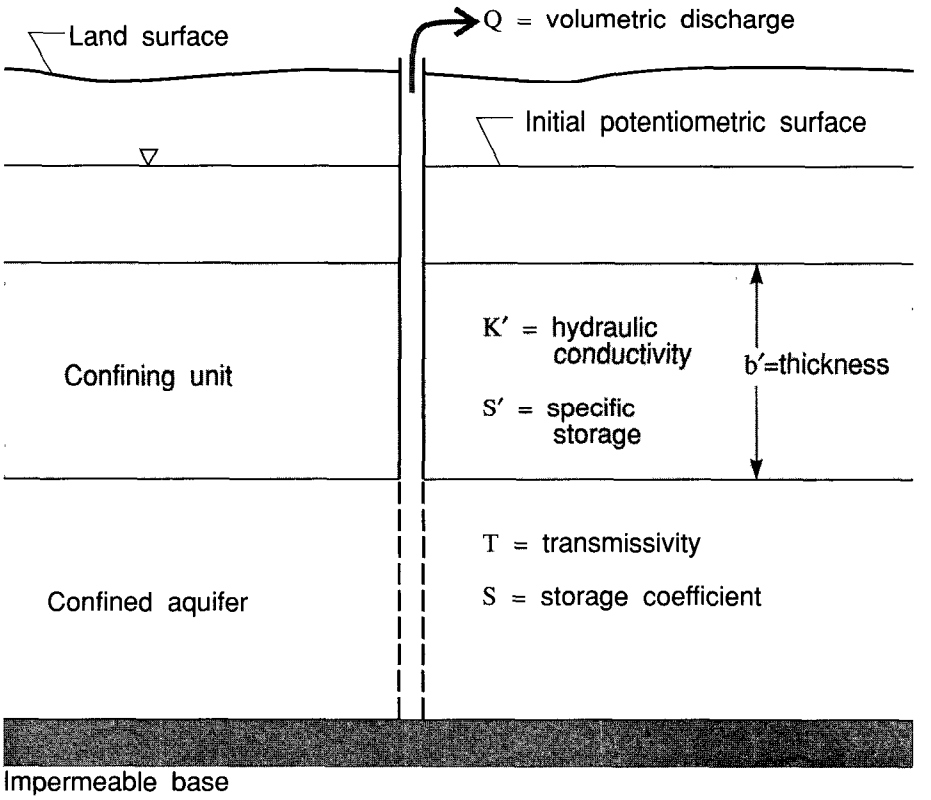

Figure 20. Geometry used to simulate the effects of transient leakage on drawdown near a pumped well.

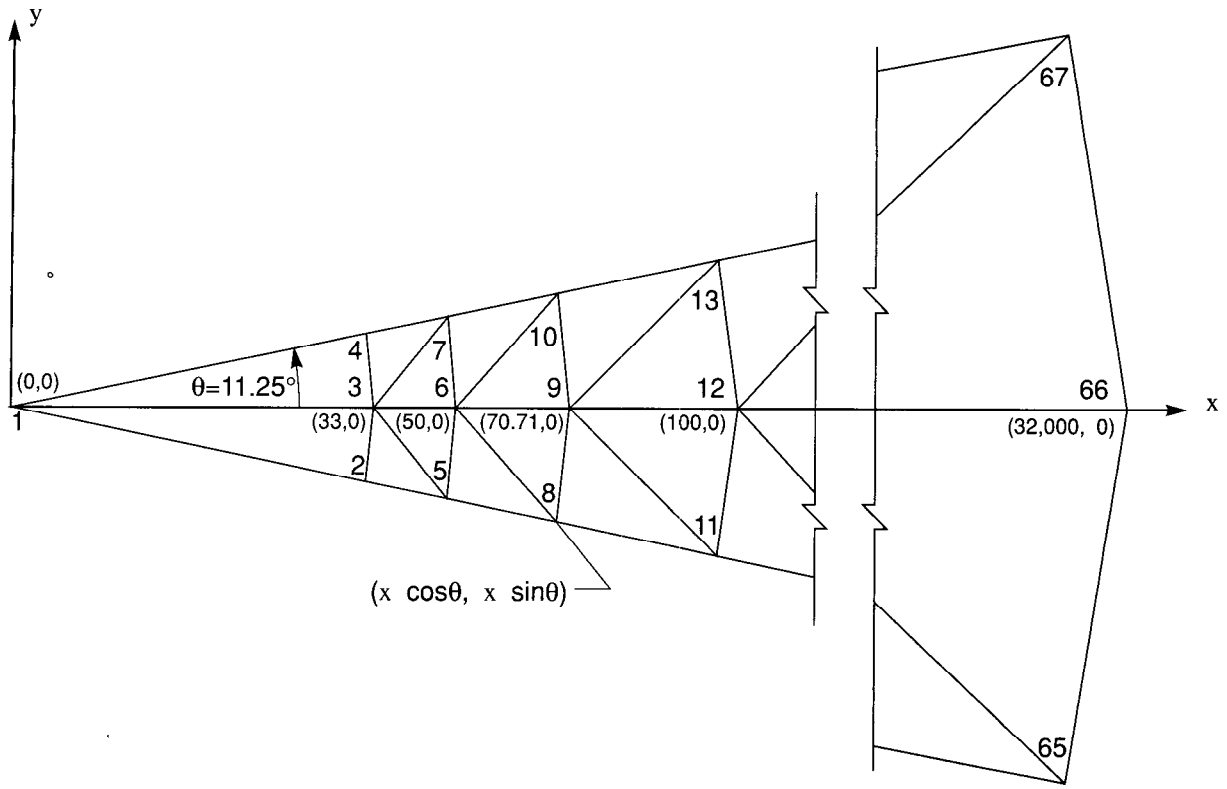

Figure 21. Finite-element mesh used to simulate the effects of transient leakage on drawdown near a pumped well.

from the pumped well by the factor $\sqrt{2}$ starting at 50 feet (figure 21). The (x,y) coordinates of nodes that are offset from the x axis by 11.25 degrees (figure 21) are computed from the x coordinate of the nodes located on the x axis as (x cos θ, x sin θ), where θ = ±11.25 degrees.

Hydraulic heads are specified at nodes 65, 66, and 67 along the external model boundary that is 32,000 feet from the pumped well. This boundary is beyond the radius of influence of the pumped well during the simulation period. Because the flow system exhibits radial symmetry, element sides that are oriented in the radial direction from the well represent flow lines; hence, there is no flow across these element sides. Other characteristics of the problem are

$$T = 10^5 \text{ ft}^2/\text{d},$$
$$S = 1.25 \times 10^{-4},$$
$$Q = 1{,}256{,}637 \text{ ft}^3/\text{d},$$
$$h(x,y,0) = 0 \text{ ft},$$
$$h(r = 32{,}000 \text{ ft}, t) = 0 \text{ ft}$$

for the aquifer and

$$K' = 10 \text{ ft/d},$$
$$b' = 400 \text{ ft},$$
$$S' = 0.008$$

for the confining unit. The head above the confining unit is held constant at 0 feet for the simulation period.

Pumpage is simulated for 0.10417 day (about 15 minutes) using 87 time elements. An initial time-element size of 2×10^{-8} day was selected, and the other time-element sizes were generated by multiplying previous values by factors ranging from 1.0 to 1.5.

Computed values of $4\pi Ts/Q$ versus $1/u$ at distances of 100, 300, 500, and 2,000 feet from the pumped well are compared with the type curves $H(u,\beta')$ versus $1/u$ using β' values of 0.1, 0.3, 0.5, and 2, respectively, in figure 22. The Theis solution plotted on this figure indicates the extent to which transient leakage affects drawdown. The numerical results show good agreement with the analytical solution.

MOENCH AND PRICKETT SOLUTION FOR CONVERSION FROM CONFINED TO UNCONFINED FLOW NEAR A PUMPED WELL

An analytical solution of Moench and Prickett (1972) is used to test the accuracy of MODFE for the problem of drawdown in an aquifer that converts from confined to unconfined conditions. A fully penetrating well of negligible diameter placed in a nonleaky, confined, homogeneous, and isotropic aquifer that is infinite in areal extent pumps at a constant rate Q sufficient to partially dewater the aquifer near the well (figure 23). Ground-water flow is assumed to be horizontal and obeys the Dupuit assumptions (Bear, 1979, p. 74-78) in the unconfined part of the aquifer. Changes in aquifer thickness, b, with drawdown in the unconfined part of the aquifer are assumed to be small and do not cause significant changes in transmissivity.

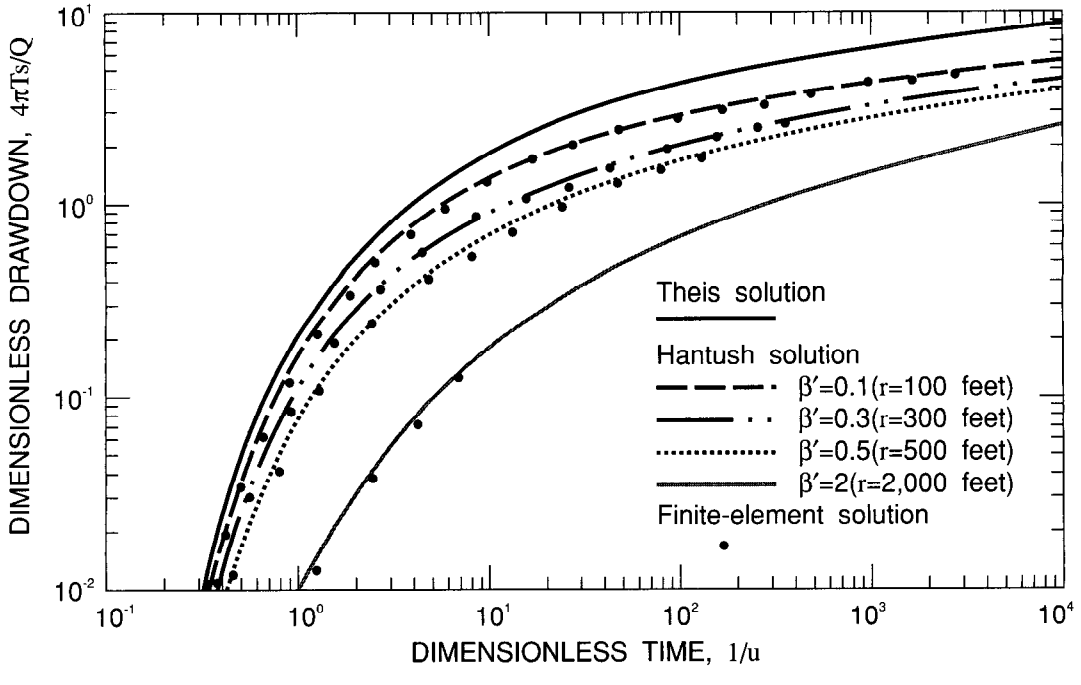

Figure 22. Hantush (1960) solution and finite-element results for the effects of transient leakage on drawdown near a pumped well.

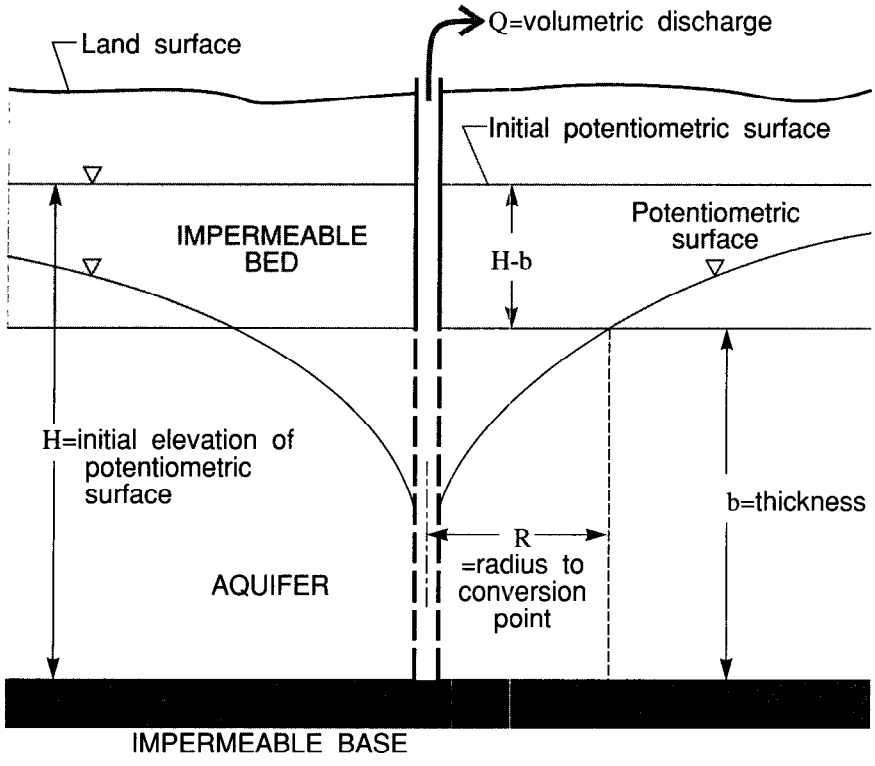

Figure 23. Geometry used to simulate the effects of conversion from confined to unconfined flow near a pumped well.

Solutions for total drawdown in the unconfined part of the aquifer, s_1, and in the confined part, s_2, are given by

$$s_1 = \frac{Q}{4\pi T}\left[W(u_1,v) + \frac{4\pi T(H-b)}{Q}\right],$$

and

$$s_2 = \frac{Q}{4\pi T}\left\{e^{v[(\alpha_1/\alpha_2)-1]}W\left(u_2\right)\right\},$$

where

$$u_1 = \frac{r^2 S_y}{4Tt},$$

$$u_2 = \frac{r^2 S}{4Tt},$$

$$v = \frac{R^2 S_y}{4Tt},$$

S_y is the specific yield, S is the storage coefficient, α_1/α_2 [0] is the aquifer-diffusivity ratio $(T/S_y)/(T/S)$, or S/S_y, and R is the radial distance from the pumped well to where conversion takes place. $W(u_2)$ is the well function used for the Theis solution and $W(u_1,v) = W(u_1)-W(v)$.

The aquifer problem is simulated using Cartesian coordinates, and the finite-element mesh is the same as used by Wilson and others (1979, p. 95-101) for a similar test problem, except that their mesh terminated at

r = 8,000 feet whereas the mesh used here extends to r = 32,000 feet. The 22.5-degree wedge of the aquifer region is subdivided into 68 triangular elements and 52 nodes (figure 24) such that the node spacing expands in the radial direction by a factor of $\sqrt{2}$ starting at 125 feet from the well. Time elements range in size from the initial value of 5×10^{-5} days to a final value of 30 days and are expanded by factors of 1.0 for the first four elements to approximately 1.5 afterward; 44 time elements were used. Other characteristics of the problem are

$$K = 26.73 \text{ ft/d},$$
$$b = 100 \text{ ft},$$
$$S_y = 0.1,$$
$$S = 0.0001,$$
$$Q = 33{,}591 \text{ ft}^3/\text{d},$$
$$h(x,y,0) = 0 \text{ ft},$$
$$H = 0 \text{ ft}.$$

A Cauchy-type boundary is placed along the element sides at 32,000 feet. Because the influence of the pumped well on the aquifer extends beyond this radial distance and the analytical solution assumes that the aquifer has an infinite areal extent, the Cauchy-type boundary is used to simulate the part of the aquifer that is influenced by the pumped well but is not represented by the finite-element mesh. It allows flow across the artificial model boundary from the aquifer region that is external to the mesh, and allows drawdowns to be computed at the model boundary.

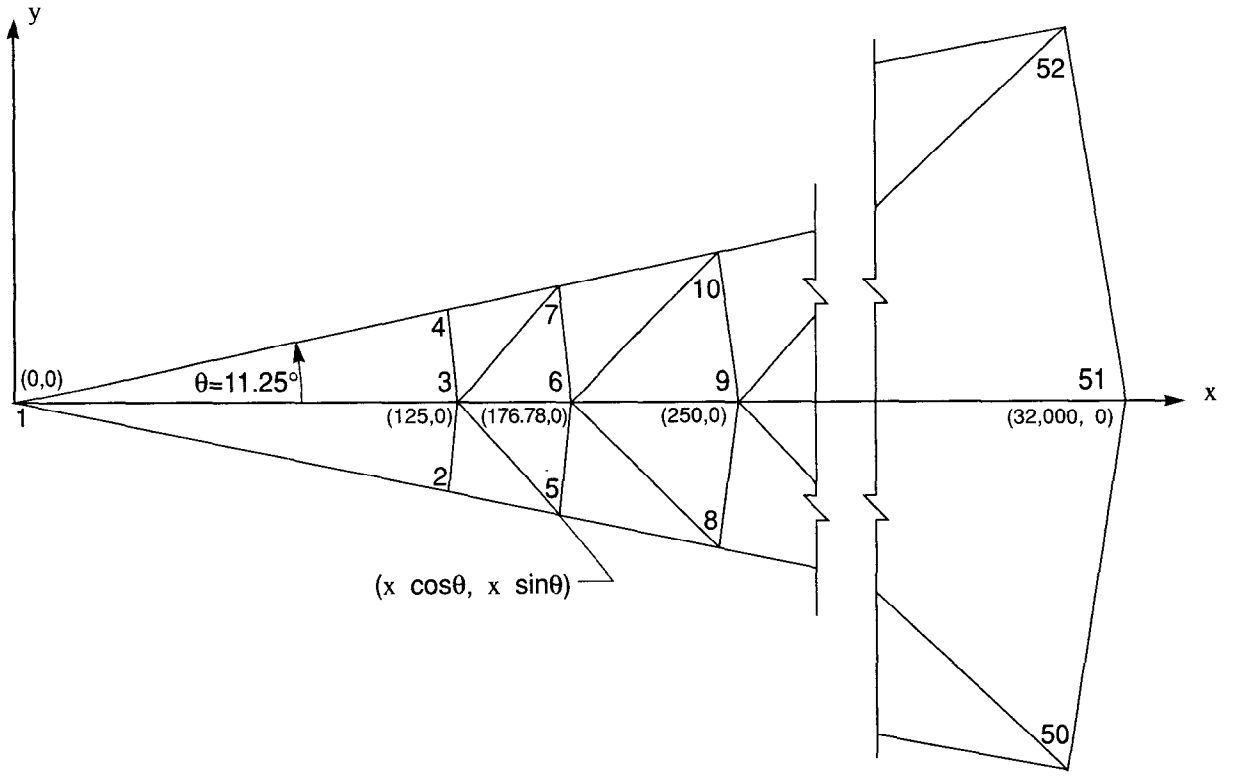

Figure 24. Finite-element mesh used to simulate the effects of conversion from confined to unconfined flow near a pumped well.

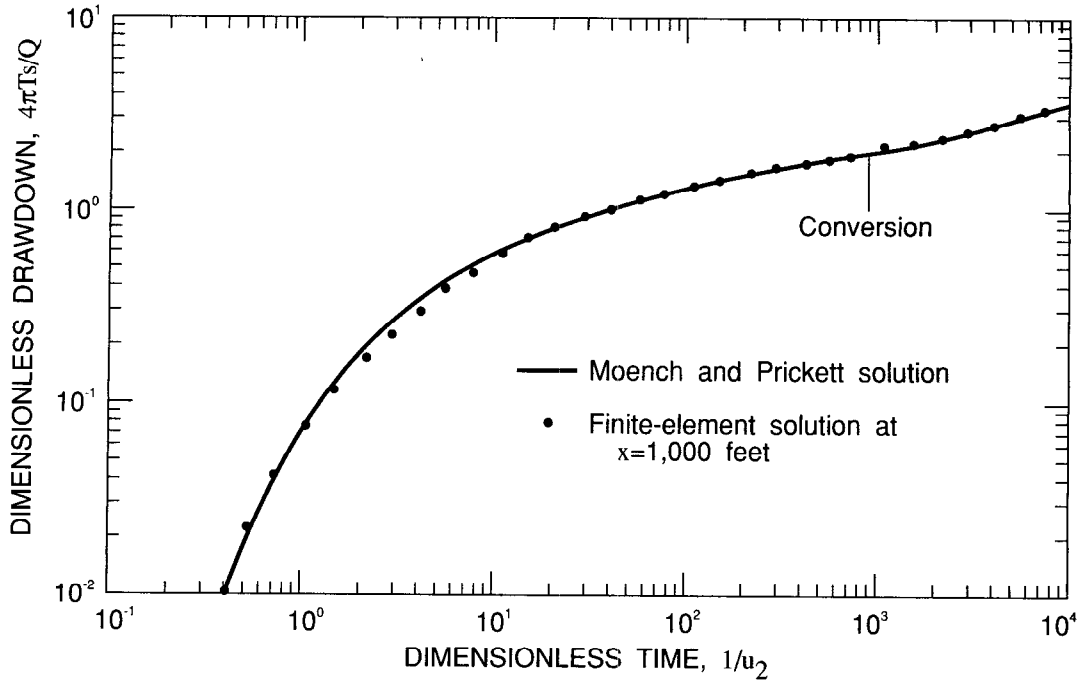

Figure 25. Moench and Prickett (1972) solution and finite-element results for conversion from confined to unconfined flow near a pumped well.

The specified head H_B (equation (4)) for the Cauchy-type boundary was located 200,000 feet from the pumped well. It is assumed that all drawdown in the infinite aquifer occurs within this distance. The coefficient α was obtained by assuming that flow beyond 32,000 feet is governed by the steady-state flow equation with known-head boundary conditions of $\hat{h}(t)$ at $r = 32{,}000$ feet and $H_B = 0$ at $r = 200{,}000$ feet. Therefore, by using the appropriate solution to the steady-state flow equation (Bear, 1979, p. 306, equation (8-7)) and equation (4),

$$q_n = T \left.\frac{\partial h}{\partial r}\right|_{r = 32{,}000} = \frac{T\left(\hat{h} - H_B\right)}{\ln\left(\frac{32{,}000}{200{,}000}\right)} \quad \frac{1}{32{,}000}$$

$$= \alpha\left(H_B - \hat{h}\right),$$

so that, because $T = 2{,}673$ ft^2/d, $\alpha = 0.04558$ ft/d.

Computed drawdowns at a radial distance of 1,000 feet from the pumped well were compared with the analytical solution. Values of dimensionless drawdown, $4\pi Ts/Q$, and dimensionless time, $1/u_2$, were computed from the simulation results and are plotted in figure 25 along with the type curves of the analytical solution. Values for $e^{v[(\alpha_1/\alpha_2)-1]}W(u_2)$ versus $1/u_2$ were plotted for drawdowns less than 2 feet (before conversion), and values of $\left[W(u_1,v) + 2\right]$ versus $1/u_2$ were plotted for drawdowns greater than 2 feet (after conversion). The numerical results are in good agreement with the analytical solution, and are better than the results of Wilson and others (1979, p. 99) because they specified $H_B = 0$ at $r = 8{,}000$ feet, which did not allow drawdown to propagate beyond 8,000 feet as it should have.

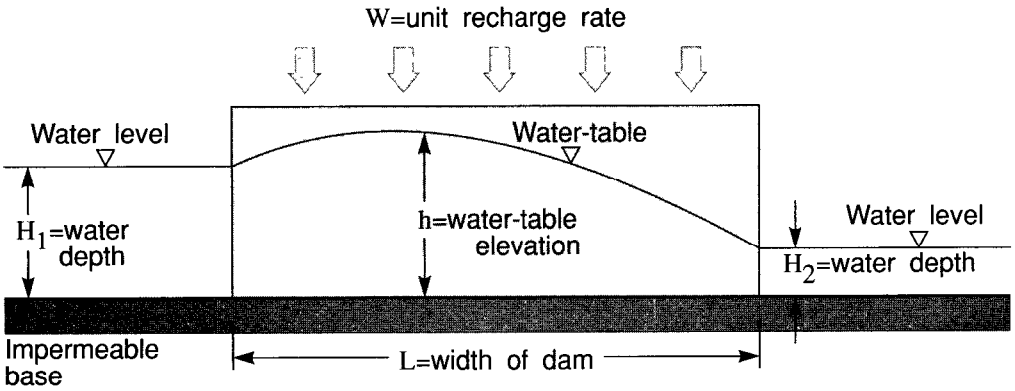

Figure 26. Cross section of steady-state flow through a dam with areal recharge.

STEADY-STATE FLOW THROUGH A DAM WITH AREAL RECHARGE

A straight dam with vertical faces 50 meters wide and 100 meters long maintains a water level of 8 meters on one side and 2 meters on the other side (figure 26). The hydraulic conductivity, K, of the earth material in the dam is 10^{-6} m/s and areal recharge, W, is applied to the surface of the dam at the rate of 4.8×10^{-8} m/s (figure 27). By making the Dupuit assumptions for unconfined flow, the solution for the height, h, of the water table in the dam can be obtained as the Dupuit parabola (see Verruijt, 1970, p. 51-57),

$$h^2 = H_1^2 - \left(H_1^2 - H_2^2\right)\frac{x}{L} + \frac{W}{K}x(L - x),$$

where x is the horizontal distance along the width L of the dam and the water levels H_1 and H_2 on either side of the dam are

$$H_1 = 8 \text{ meters}, \quad x = 0 \text{ meters},$$

$$H_2 = 2 \text{ meters}, \quad x = L = 50 \text{ meters}.$$

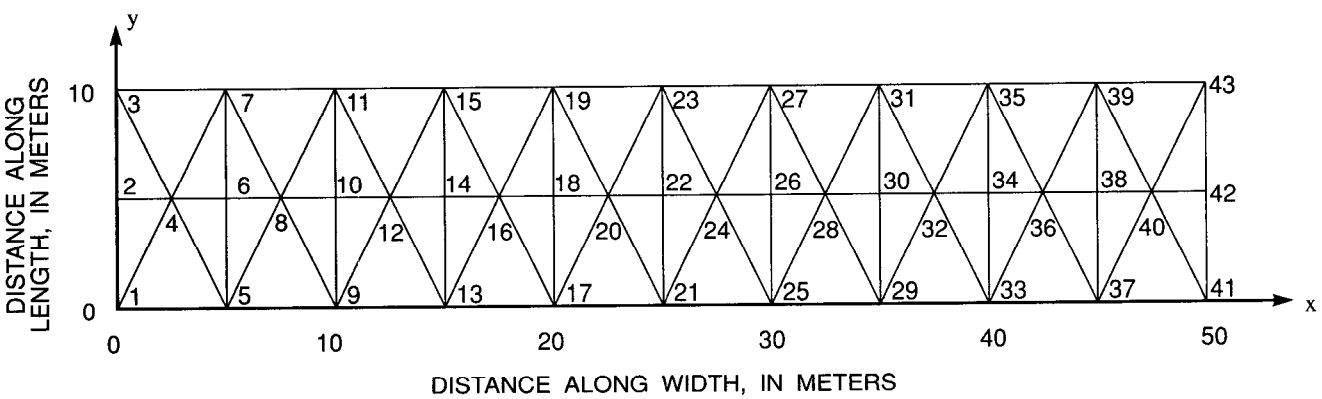

Figure 27. Finite-element mesh used to simulate steady-state flow through a dam with areal recharge.

Because ground-water flow is virtually one-dimensional through the dam, the entire 100-meter length need not be simulated. Instead, a 10-meter-long section of the dam is represented by a finite-element mesh consisting of 60 triangular elements and 43 nodes (figure 27). No-flow boundaries are placed along the element sides that are parallel to the x axis at y = 0 meters and y = 10 meters, because ground-water flow is parallel to these boundaries. Specified-head boundaries are located along the lines x = 0 meters and x = 50 meters in order to maintain the height of the water levels at the values given for H_1 and H_2, respectively. Areally distributed recharge is applied over the entire model area.

The steady-state solution for the water-table height provided by MODFE is plotted along with the analytical solution in figure 28. The solution by MODFE is in close agreement with the analytical solution.

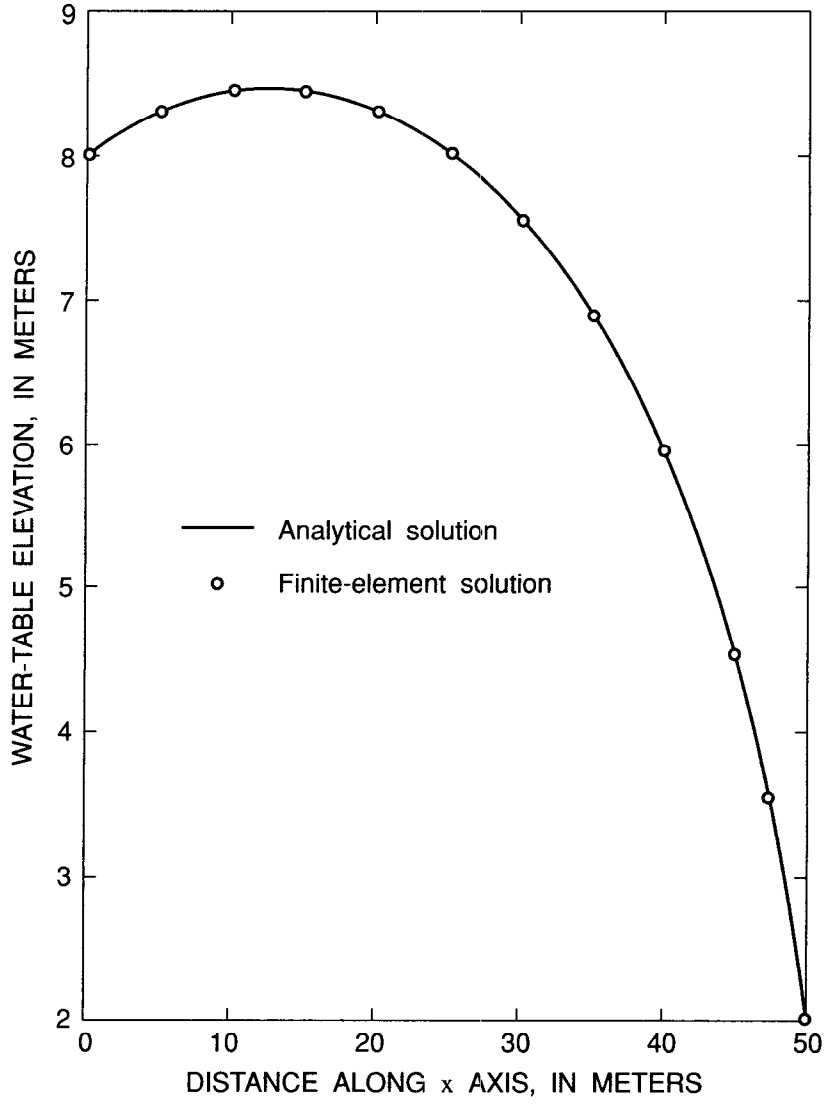

Figure 28. Analytical solution (Dupuit parabola) and finite-element results for steady-state flow through a dam with areal recharge.

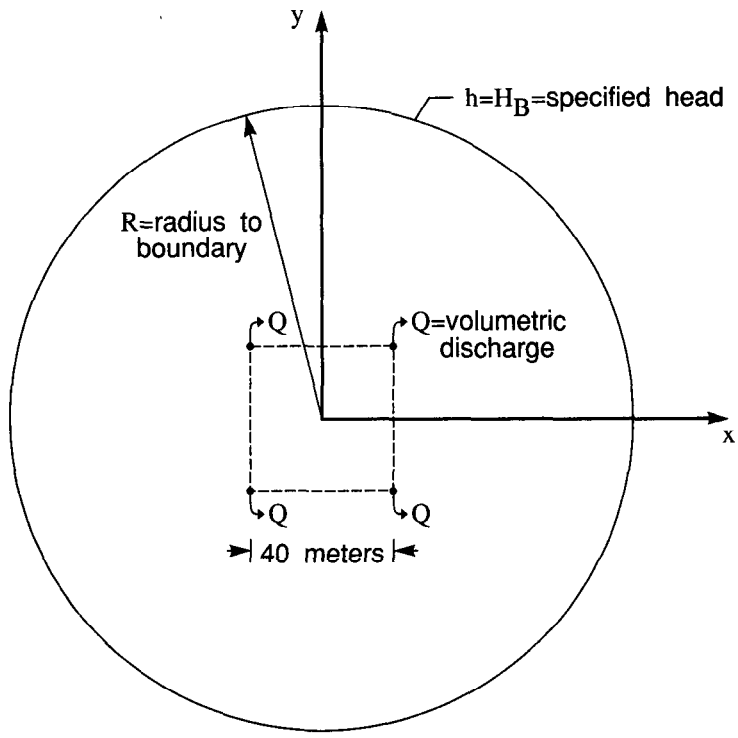

Figure 29. Geometry for two-dimensional steady-state flow in an unconfined aquifer.

TWO-DIMENSIONAL STEADY-STATE FLOW IN AN UNCONFINED AQUIFER

The flow problems described previously for testing the accuracy of MODFE have one-dimensional solutions, even though MODFE solved these problems in two dimensions. This flow problem tests the ability of MODFE to accurately compute steady-state water levels in an unconfined aquifer for a problem that has an analytical solution in two dimensions.

The problem used in this simulation is taken from Verruijt (1970, Problem 6.2) where four wells pumped at the same rate (1.196×10^{-6} m^3/s) are located at the corners of a 40-meter square in an unconfined aquifer (figure 29). The square represents a construction site where the water level is to be maintained 4 meters below the original water table, which is 10 meters above the impermeable base. The aquifer is homogeneous and isotropic with a hydraulic conductivity, K, of 10^{-7} m/s, an initial thickness of 10 meters, and an external radius, R, of 2,000 meters, measured from the center of the square. Beyond R the drawdown is zero.

The solution for the aquifer head, h, is given by Verruijt (1970, p. 66) as

$$h = \left[H_B^2 + \frac{1}{\pi K} \sum_{j=1}^{4} Q_j \ln \frac{\sqrt{(x - x_j)^2 + (y - y_j)^2}}{R} \right]^{1/2}$$

where H_B is the specified head (10 meters) at the radius R and Q_j is the volumetric discharge from well j located at the point (x_j, y_j) in the aquifer.

Because the wells are pumped at the same rate and are regularly spaced about the center of the square (see figure 29), the flow problem can be simulated in the 45-degree wedge shown in figure 30. The origin of the wedge is the center of the square, and one of the four pumped wells is placed at the point (20 meters, 20 meters) in the wedge. No-flow boundaries are located along the x axis and the line y = x, and a specified-head boundary (H_B = 10 meters) is located at a distance of 2,000 meters from the center of the square.

The aquifer region is subdivided by a finite-element mesh consisting of 94 triangular elements and 67 nodes (figure 30). Results from the nonlinear steady-state simulation and the analytical solution are presented in figure 31. The simulated results show good agreement with the analytical solution.

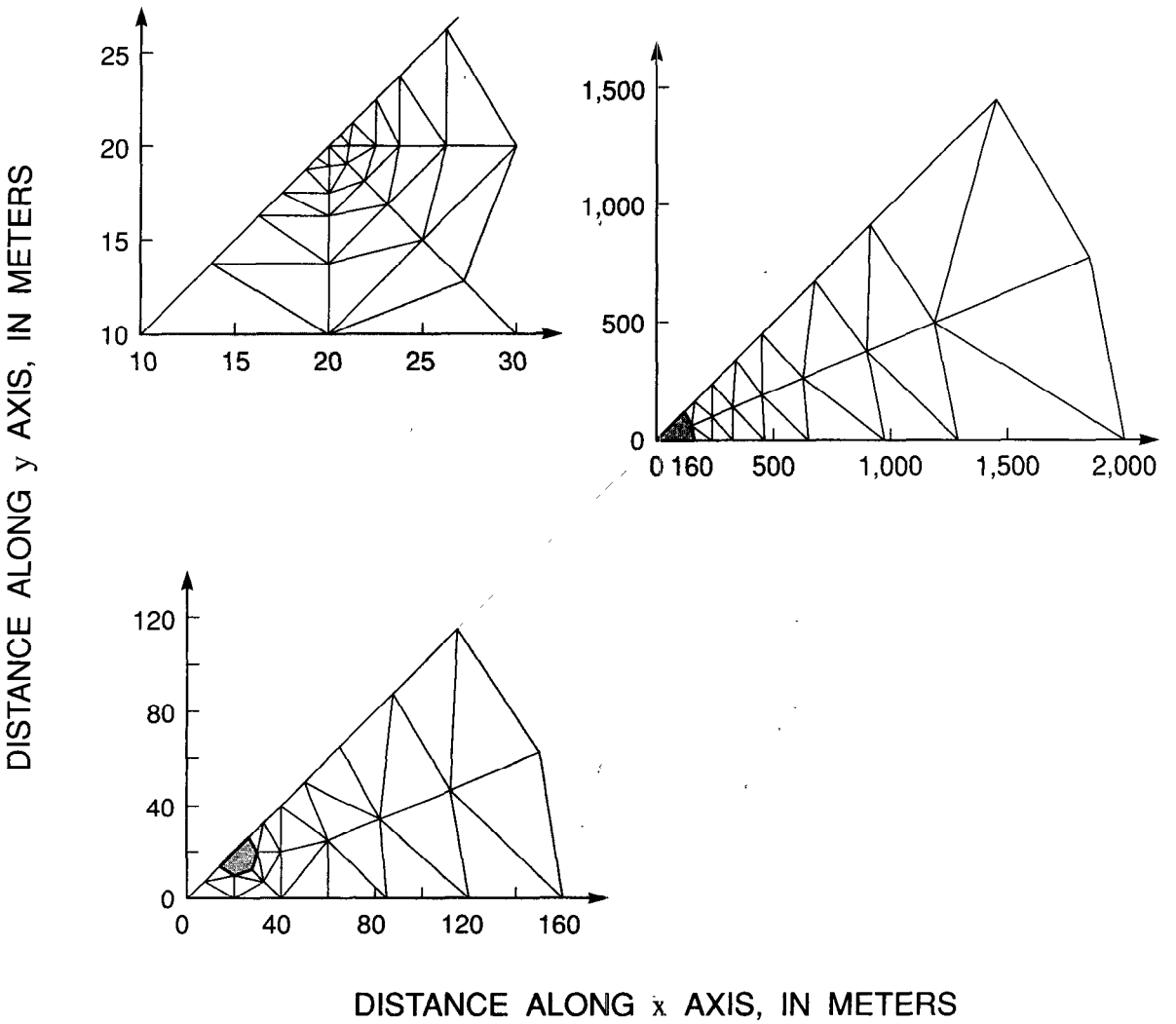

Figure 30. Finite-element mesh used to simulate two-dimensional steady-state flow in an unconfined aquifer.

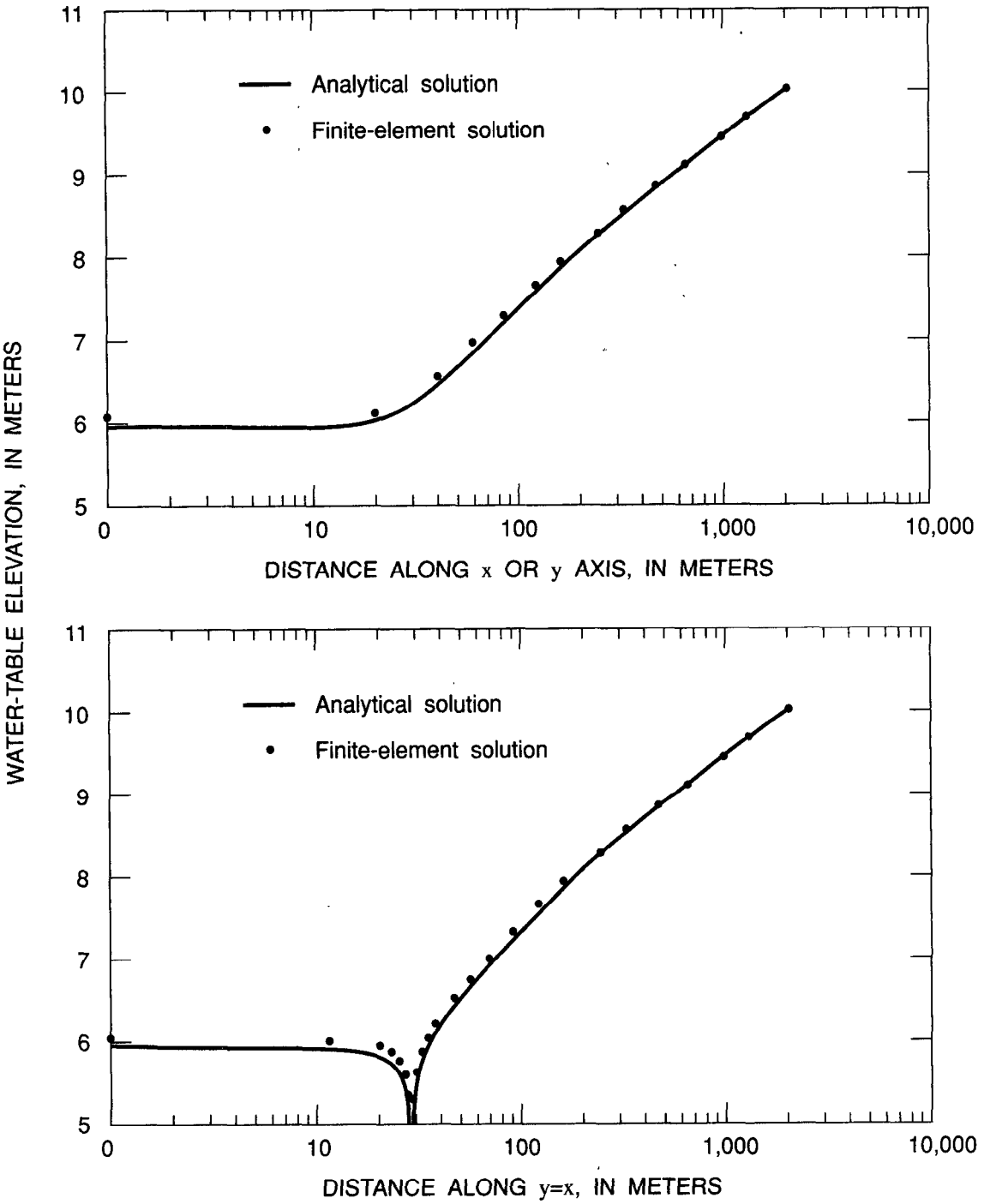

Figure 31. Analytical solution and finite-element results for two-dimensional steady-state flow in an unconfined aquifer.

SUMMARY

The two-dimensional steady- and unsteady-state equations for groundwater flow in a heterogeneous, anisotropic aquifer were approximately solved with finite-element techniques. Spatial finite elements are triangular with two-dimensional linear basis functions and time elements are linear, with

one-dimensional linear basis functions. Finite-element equations were derived by minimizing a functional of the difference between true and approximate hydraulic heads and are equivalent to finite-element equations obtained by either classical variational or Galerkin methods. Variable directions of anisotropy are incorporated by rotating the coordinate system locally so that the rotated coordinates are aligned with the local principal directions of the transmissivity tensor. For unsteady-state problems, a mass balance is computed at the end of each time element. Computed flow components include accumulation or depletion of water in storage, flow across confining beds, flow across specified-head boundaries, flow across specified-flow boundaries, and flow across head-dependent flow boundaries. For steady-state problems, the mass balance, excluding the storage component, is computed at the end of the simulation.

The basic finite-element equations include the following processes: confined flow; leakage through rigid confining beds; specified areal and point recharge and discharge; and specified-flow, specified-head, or head-dependent boundary conditions. Extensions of these equations allow for unconfined flow using the Dupuit assumption, decreases of aquifer thickness to zero and increases from zero (termed drying of nodes), conversions from confined to unconfined flow and vice versa, point head-dependent discharge from springs and drainage wells, areal head-dependent leakage combined with aquifer dewatering, areal head-dependent discharge from evapotranspiration, line head-dependent leakage combined with aquifer dewatering for narrow rivers, and transient leakage from confining beds. Except for transient leakage, all of these extensions are nonlinear.

The finite-element equations were also formulated using axisymmetric cylindrical coordinates to allow analysis of problems involving axisymmetric flow in multiaquifer systems. Boundary conditions are the same as for the two-dimensional Cartesian versions, but for radial flow the principal directions of the hydraulic conductivity tensor are assumed to be the radial and vertical directions. None of the extensions can be used in this case.

Matrix solution techniques for the finite-element equations include the direct symmetric-Doolittle method, which can be efficient for small to medium problems (less than about 500 nodes), and the iterative modified incomplete-Cholesky conjugate-gradient (MICCG) method, which is more efficient for larger problems (more than about 500 nodes). Nonlinear unsteady-state problems are solved using a predictor-corrector method that can employ either the direct or MICCG method to solve both the predictor and corrector equations. Nonlinear steady-state problems are solved using an iterative method that can also employ either matrix solution method. Use of MICCG for nonlinear steady-state problems yields an inner MICCG iteration loop and an outer iteration loop on the nonlinearity. Because the inner loop converges in progressively fewer iterations as the outer loop converges, MICCG is recommended for these problems.

The accuracy of the finite-element solution method was evaluated using five test problems for which analytical solutions are available: radial flow to a well in a homogeneous, infinite, nonleaky, confined aquifer; radial flow to a well in a homogeneous, infinite, confined aquifer with transient leakage; radial flow to a well in a homogeneous, infinite, nonleaky aquifer undergoing conversion from confined to unconfined flow; one-dimensional, unconfined, steady-state flow through a dam with areal recharge; and two-dimensional, unconfined, steady-state flow to a group of drainage wells. All problems except the first were solved using Cartesian coordinates. All numerical solutions are in good agreement with the analytical solutions.

REFERENCES CITED

Bear, Jacob, 1979, Hydraulics of groundwater: New York, McGraw-Hill, 569 p.

Beckman, F.S., 1967, The solution of linear systems by the conjugate gradient method, in Ralston, Anthony, and Wilf, H.S., Mathematical methods for digital computers, v. 1: New York, John Wiley, p. 62-72.

Bettencourt, J.M., Zienkiewicz, O.C., and Cantin, G., 1981, Consistent use of finite elements in time and the performance of various recurrence schemes for the heat diffusion equation: International Journal for Numerical Methods in Engineering, v. 17, p. 931-938.

Briggs, J.E., and Dixon, T.N., 1968, Some practical considerations in the numerical solution of two-dimensional reservoir problems: Society of Petroleum Engineers Journal, v. 8, no. 2, p. 185-194.

Carslaw, H.S., and Jaeger, J.C., 1959, Conduction of heat in solids: Oxford, Great Britain, Clarendon, 510 p.

Concus, Paul, Golub, G.H., and O'Leary, D.P., 1975, A generalized conjugate gradient method for the numerical solution of elliptic partial differential equations: Berkeley, Calif., Lawrence Berkeley Publication LBL-4604, 24 p.

Cooley, R.L., 1971, A finite difference method for unsteady flow in variably saturated porous media: Application to a single pumping well: Water Resources Research, v. 7, no. 6, p. 1607-1625.

----- 1972, Numerical simulation of flow in an aquifer overlain by a water-table aquitard: Water Resources Research, v. 8, no. 4, p. 1046-1050.

----- 1974, Finite element solutions for the equations of ground-water flow: Center for Water Resources Research, Desert Research Institute, University of Nevada System, Reno, Technical Report Series H-W, Hydrology and Water Resources Publication No. 18, 134 p.

----- 1983, Some new procedures for numerical solution of variably saturated flow problems: Water Resources Research, v. 19, no 5, p. 1271-1285.

Cooley, R.L., and Naff, R.L., 1990, Regression modeling of ground-water flow: U.S. Geological Survey Techniques of Water-Resources Investigations, Book 3, Chapter B4, 232 p.

Crank, J., and Nicolson, P., 1947, A practical method for numerical evaluation of solutions of partial differential equations of the heat-conduction type: Proceedings of the Cambridge Philosophical Society, v. 43, p. 50-67.

Desai, C.S., and Abel, J.F., 1972, Introduction to the finite element method: New York, Van Nostrand Reinhold, 477 p.

Douglas, Jim, Jr., and Jones, B.F., 1963, On predictor-corrector methods for nonlinear parabolic differential equations: Journal for the Society of Industrial and Applied Mathematics, v. 11, p. 195-204.

Fox, Leslie, 1965, An introduction to numerical linear algebra: New York, Oxford, 327 p.

Gambolati, Giuseppe, and Volpi, Giampiero, 1982, Analysis of performance of the modified conjugate gradient method for solution of sparse linear sets of finite element equations, in Gallagher, R.H., Norrie, D.H., Oden, J.T., and Zienkiewicz, O.C., eds., Finite Elements in Fluids, v. 4: 3rd International Conference on Finite Elements in Flow Problems held at Banff, Alberta, Canada, 10-13 June, 1980, John Wiley, p. 256-264.

Gresho, P.M., Lee, R.L., and Sani, R.L., 1976, Advection-dominated flows, with emphasis on the consequences of mass lumping: International Centre for Computer Aided Design, Second International Symposium on Finite Element Methods in Flow Problems held at Santa Margherita Ligure, Italy, June 14-June 18, 1976, p. 745-756.

Gustafsson, Ivar, 1978, A class of first order factorization methods: BIT, v. 18, no. 2, p. 142-156.

----- 1979, On modified incomplete Cholesky factorization methods for the solution of problems with mixed boundary conditions and problems with discontinuous material coefficients: International Journal for Numerical Methods in Engineering, v. 14, p. 1127-1140.
Hantush, M.S., 1960, Modification of the theory of leaky aquifers: Journal of Geophysical Research, v. 65, no. 11, p. 3713-3725.
Herrera, Ismael, 1970, Theory of multiple leaky aquifers: Water Resources Research, v. 6, no. 1, p. 185-193.
----- 1974, Integrodifferential equations for systems of leaky aquifers and applications, 2, Error analysis of approximate theories: Water Resources Research, v. 10, no. 4, p. 811-820.
Herrera, Ismael, and Rodarte, Leopoldo, 1973, Integrodifferential equations for systems of leaky aquifers and applications, 1, The nature of approximate theories: Water Resources Research, v. 9, no. 4, p. 995-1005.
Herrera, Ismael, and Yates, Robert, 1977, Integrodifferential equations for systems of leaky aquifers and applications, 3, A numerical method of unlimited applicability: Water Resources Research, v. 13, no. 4, p. 725-732.
Hohn, F.E., 1964, Elementary matrix algebra (2d ed.): New York, Macmillan, 395 p.
Lohman, S.W., 1972, Ground-water hydraulics: U.S. Geological Survey Professional Paper 708, 70 p.
Manteuffel, T.A., 1980, An incomplete factorization technique for positive definite linear systems: Mathematics of Computation, v. 34, no. 150, p. 473-497.
McCracken, D.D., and Dorn, W.S., 1964, Numerical methods and FORTRAN programming: New York, John Wiley, 457 p.
Meijerink, J.A., and van der Vorst, H.A., 1977, An iterative solution method for linear systems of which the coefficient matrix is a symmetric M-matrix: Mathematics of Computation, v. 31, no. 137, p. 148-162.
Moench, A.F., and Prickett, T.A., 1972, Radial flow in an infinite aquifer undergoing conversion from artesian to water table conditions: Water Resources Research, v. 8, no. 2, p. 494-499.
Narasimhan, T.N., Neuman, S.P., and Witherspoon, P.A., 1978, Finite element method for subsurface hydrology using a mixed explicit-implicit scheme: Water Resources Research, v. 14, no. 5, p. 863-877.
Neuman, S.P., and Witherspoon, P.A., 1969, Theory of flow in a confined two-aquifer system: Water Resources Rsearch, v. 5, no. 4, p. 803-816.
Norrie, D.H., and de Vries, Gerard, 1973, The finite element method: New York, Academic, 322 p.
Pinder, G.F., and Gray, W.G., 1977, Finite element simulation in surface and subsurface hydrology: New York, Academic, 295 p.
Prickett, T.A., and Lonnquist, L.G., 1971, Selected digital computer techniques for groundwater resource evaluation: Illinois State Water Survey, Bulletin 55, 62 p.
Remson, Irwin, Hornberger, G.M., and Molz, F.J., 1971, Numerical methods in subsurface hydrology: New York, Wiley-Interscience, 389 p.
Segerlind, L.J., 1976, Applied finite element analysis: New York, John Wiley, 422 p.
Smith, G.D., 1965, Numerical solution of partial differential equations: New York, Oxford, 179 p.
Spiegel, M.R., 1959, Theory and problems of vector analysis: New York, Schaum, 225 p.
Torak, L.J., 1992a, A MODular Finite-Element model (MODFE) for areal and axisymmetric ground-water flow problems, part 1: Model description and user's manual: U.S. Geological Survey Open-File Report 90-194.

----- 1992b, A MODular Finite-Element model (MODFE) for areal and axisymmetric ground-water flow problems, part 3: Design philosophy and programming details: U.S. Geological Survey Open-File Report 91-471.
Trescott, P.C., Pinder, G.F., and Larson, S.P., 1976, Finite-difference model for aquifer simulation in two dimensions with results of numerical experiments: U.S. Geological Survey Techniques of Water-Resources Investigations, Book 7, Chapter C1, 116 p.
Varga, R.S., 1962, Matrix iterative analysis: Englewood Cliffs, N.J., Prentice-Hall, 322 p.
Verruijt, A., 1970, Theory of groundwater flow: New York, Gordon and Breach, 190 p.
Wang, H.F., and Anderson, M.P., 1982, Introduction to groundwater modeling; Finite difference and finite element methods: San Francisco, W.H. Freeman, 237 p.
Wilson, J.L., Townley, L.R., and Sa da Costa, A., 1979, Mathematical development and verification of a finite element aquifer flow model AQUIFEM-1: Massachusetts Institute of Technology, Technological Planning Program, TAP Report 79-2, 114 p.
Wong, Y.S., 1979, Pre-conditioned conjugate gradient methods for large sparse matrix problems, in Lewis, R.W., and Morgan, K., eds., Numerical methods in thermal problems: Proceedings of the First International Conference held at University College, Swansea, England, 2-6 July, 1979, Pineridge Press, p. 967-979.
Zienkiewicz, O.C., 1971, The finite element method in engineering science: London, McGraw-Hill, 521 p.
Zienkiewicz, O.C., Mayer, Paul, and Cheung, Y.K., 1966, Solution of anisotropic seepage by finite elements: Journal of the Engineering Mechanics Division, Proceedings of the American Society of Civil Engineers, v. 92, no. EM1, p. 111-120.

APPENDIX A

APPENDIX A

It is shown here that

$$\sum_{e_i}\int_0^{\Delta t_{n+1}} \sigma_{n+1}\left\{\iint_{\Delta^e}\left[N_i^e\left(S\frac{\partial h}{\partial t} - R(H - h) - W - P\right) + \frac{\partial N_i^e}{\partial x}\left(T_{xx}\frac{\partial h}{\partial x} + T_{xy}\frac{\partial h}{\partial y}\right)\right.\right.$$

$$\left.\left. + \frac{\partial N_i^e}{\partial y}\left(T_{yx}\frac{\partial h}{\partial x} + T_{yy}\frac{\partial h}{\partial y}\right)\right]dxdy - \int_{C_2^e} N_i^e\left[q_B + \alpha\left(H_B - h\right)\right]dC\right\}dt' = 0. \quad \text{(A1)}$$

To simplify notation, the generalized Darcy's law (Bear, 1979, p. 71) is used to replace the terms involving transmissivity. That is,

$$q_x = -T_{xx}\frac{\partial h}{\partial x} - T_{xy}\frac{\partial h}{\partial y} \quad \text{(A2)}$$

and

$$q_y = -T_{yx}\frac{vh}{\partial x} - T_{yy}\frac{vh}{\partial y} \quad \text{(A3)}$$

are used to write equation (A1) as

$$\sum_{e_i}\int_0^{\Delta t_{n+1}} \sigma_{n+1}\left\{\iint_{\Delta^e}\left[N_i^e\left(S\frac{\partial h}{\partial t} - R(H - h) - W - P\right) - \frac{\partial N_i^e}{\partial x}q_x - \frac{\partial N_i^e}{\partial y}q_y\right]dxdy\right.$$

$$\left. - \int_{C_2^e} N_i^e\left[q_B + \alpha\left(H_B - h\right)\right]dC\right\}dt' = 0. \quad \text{(A4)}$$

To initiate the proof, equations (A2) and (A3) are substituted into equation (1), which is then multiplied by $\sigma_{n+1}N_i^e$ and integrated over spatial element e and time element n+1 to obtain

$$\int_0^{\Delta t_{n+1}} \sigma_{n+1}\left\{\iint_{\Delta^e} N_i^e\left(S\frac{\partial h}{\partial t} - R(H - h) - W - P\right)dxdy\right\}dt'$$

$$= -\int_0^{\Delta t_{n+1}} \sigma_{n+1}\left\{\iint_{\Delta^e} N_i^e\left(\frac{\partial q_x}{\partial x} + \frac{\partial q_y}{\partial y}\right)dxdy\right\}dt'. \quad \text{(A5)}$$

Next, a result from vector calculus known as Green's first identity (Spiegel, 1959, p. 107) is used to modify the right side of equation (A5).

If q_x, q_y, and N_i^e are continuous and have continuous derivatives in element e, then

$$\int_{\Delta^e}\int N_i^e\left(\frac{\partial q_x}{\partial x} + \frac{\partial q_y}{\partial y}\right)dxdy = -\int_{\Delta^e}\int\left(\frac{\partial N_i^e}{\partial x}q_x + \frac{\partial N_i^e}{\partial y}q_y\right)dxdy - \int_{C^e} N_i^e q_n dC, \qquad (A6)$$

where q_n is the component of the flow vector (q_x, q_y) that is normal to the element boundary and is positive for inflow, and C^e is the boundary of element e. Substitution of equation (A6) into equation (A5) and rearrangement yields

$$\int_0^{\Delta t_{n+1}} \sigma_{n+1}\left\{\int_{\Delta^e}\int\left[N_i^e\left(S\frac{\partial h}{\partial t} - R(H - h) - W - P\right) - \frac{\partial N_i^e}{\partial x}q_x - \frac{\partial N_i^e}{\partial y}q_y\right]dxdy - \int_{C^e} N_i^e q_n dC\right\}dt' = 0. \qquad (A7)$$

The integral over the element boundary C^e can be split into two integrals: the integral over a Cauchy-type boundary and the integral over the remaining side(s), so that

$$\int_{C^e} N_i^e q_n dC = \int_{C_1^e} N_i^e q_n dC + \int_{C_2^e} N_i^e\left[q_B + \alpha\left(H_B - h\right)\right]dC, \qquad (A8)$$

where C_1^e designates the side(s) that are not Cauchy-type boundaries and equation (4) was used to replace q_n in the integral over a Cauchy-type boundary.

When equation (A7) is summed over all elements in the patch for node i, all boundary integrals over C_1^e for adjacent element sides cancel because of equation (3) and the continuity of N_i^e across an element boundary. Furthermore, all boundary integrals for element sides forming the outer boundary of the patch are zero, because N_i^e is zero on these sides. Therefore, equation (A7) yields

$$\sum_{e_i}\int_0^{\Delta t_{n+1}} \sigma_{n+1}\left\{\int_{\Delta^e}\int\left[N_i^e\left(S\frac{\partial h}{\partial t} - R(H - h) - W - P\right) - \frac{\partial N_i^e}{\partial x}q_x - \frac{\partial N_i^e}{\partial y}q_y\right]dxdy - \int_{C_2^e} N_i^e\left[q_B + \alpha\left(H_B - h\right)\right]dC\right\}dt' = 0, \qquad (A9)$$

which, when written using equations (A2) and (A3) to replace q_x and q_y, is equation (A1).

NOTATION

The principal notation used in this report is given below. Certain symbols used only locally are omitted from the list for brevity.

A^e, B^e, C^e • Coefficients defined by equation (6) and used to compute the approximate solution, $\hat{h}$.

A'_m, B'_m • Coefficients defined by equations (176) and (177) and used to approximate the infinite series for transient leakage calculations.

A_m, B_m • $A_m = A'_m/\alpha_m$; $B_m = B'_m/\beta_m$.

(a'_j, b'_j) • (x,y) location of the jth point source or sink. Overbars signify that the location is given in $(\bar{x},\bar{y})$ coordinates.

a_i^e, b_i^e, c_i^e • Coefficients used in basis functions N_i^e; defined by equation (10) for Cartesian coordinates and by equation (212) for axisymmetric cylindrical coordinates. Overbars signify evaluation using $(\bar{x},\bar{y})$ coordinates.

$\underline{\underline{A}}$ • Matrix $\underline{\underline{G}} + \underline{\underline{V}}$ or the coefficient matrix defined by equation (254), depending on context. Entries are A_{ij} for $\underline{\underline{A}} = \underline{\underline{G}} + \underline{\underline{V}}$ and a_{ij} for $\underline{\underline{A}}$ as the coefficient matrix. Subscript ℓ ($\underline{\underline{A}}_\ell$) signifies evaluation of the coefficient matrix at iteration ℓ for a nonlinear steady-state problem.

$\underline{B}$ • Vector of known flows and boundary conditions, defined by equations (45) and (50) for Cartesian coordinates and by equations (45) and (229) for axisymmetric cylindrical coordinates. Entries are B_i. Subscript ℓ ($\underline{B}_\ell$) signifies evaluation at iteration ℓ for a nonlinear steady-state problem.

$\bar{\underline{B}}$ • Weighted average $\underline{B}$ over time element n+1 defined by equation (62). Entries are $\bar{B}_i$.

b • Aquifer thickness; b_i is aquifer thickness at node i, and $b_{i,n}$ is aquifer thickness at node i and time level n.

b' • Confining-unit thickness; b'_i is harmonic mean confining-unit thickness at node i defined by equation (170).

C_2^e • Side(s) of element e that are Cauchy-type boundaries.

C_{ai} • Coefficient for areal head-dependent leakage function that applies for aquifer dewatering at node i; defined by equation (119).

C_{ei} • Coefficient for areal head-dependent discharge function at node i; defined by equation (132).

C_{pi} • Coefficient for point head-dependent discharge function at node i; defined by equation (104).

C_{ri} • Coefficient for line head-dependent leakage function at node i; defined by equation (155).

c_{ii}^e • Storage coefficient term for node i of element e; defined by equation (36) for Cartesian coordinates and by equation (224) for axisymmetric cylindrical coordinates.

$C_{ii}^{(1)}, C_{ii}^{(2)}$ • Entry C_{ii} of $\underline{\underline{C}}$ for before (1) and after (2) conversion from confined to unconfined flow or vice versa.

$\underline{\underline{C}}$ • Diagonal matrix with diagonal entries defined by $C_{ii} = \sum_{e_i} c_{ii}^e$.

D_{ij} • $\sum_{e_i} d_{ij}^e$.

$\underline{\underline{D}}$ • Diagonal matrix for symmetric-Doolittle factorization of $\underline{\underline{A}}$; defined by equation (260). Entries are $1/\alpha_{ii}$.

$\tilde{\underline{\underline{D}}}$ • Diagonal matrix for incomplete-Cholesky or modified incomplete-Cholesky factorization of $\underline{\underline{A}}$; defined by equation (272) and calculated using equation (273) for incomplete-Cholesky factorization or equation (279) for modified incomplete-Cholesky factorization. Entries are $1/\tilde{\alpha}_{ii}$.

d^e_{ij} • Hydraulic-conductivity term for unconfined flow; defined by equation (72).

$\underline{d}$ • Right-hand side vector for finite-element matrix equation (254). Entries are d_i.

$\hat{e}$ • Error $h - \hat{h}$ in the approximate solution of equation (1).

e_i • Index indicating summation over elements in the patch for node i.

f_{ij} • Element of fill-in in $\underline{\underline{M}}$; defined by equation (277).

$\underline{\underline{G}}$ • Matrix defined by entries $G_{ij} = \sum_{e_i} g^e_{ij}$ for confined flow and by equation (74) for unconfined flow.

$\tilde{\underline{\underline{G}}}$ • Weighted average $\underline{\underline{G}}$ over time element n+1 defined by equation (69).

$\bar{\underline{\underline{G}}}$ • Weighted average $\underline{\underline{G}}$ over time element n+1 defined by equation (70).

$\tilde{\underline{\underline{G}}}^*$ • Matrix $\tilde{\underline{\underline{G}}}$ computed using predicted head vector $\hat{\underline{h}}^*$.

$\bar{\underline{\underline{G}}}^*$ • Matrix $\bar{\underline{\underline{G}}}$ computed using predicted head vector $\hat{\underline{h}}^*$.

g^e_{ij} • Transmissivity term defined by equations (38) (or (43)), (39), and (40) for Cartesian coordinates and by equations (226), (227), and (228) for axisymmetric cylindrical coordinates.

H • Hydraulic head at the distal side of a confining unit.

H_B • Specified head at a boundary.

H_o • Initial head (at t = 0).

H_a • Hydraulic head at the distal side of a confining unit or the stage elevation of wide river overlying an aquifer being dewatered.

H_r • Controlling head for line head-dependent leakage functions (for rivers it is the river-stage elevation).

h • True hydraulic head in the aquifer.

$\hat{h}$ • Approximate hydraulic head in the aquifer defined by equation (6); $\hat{h}_i$ is $\hat{h}$ at node i and $\hat{h}_{i,n}$ is $\hat{h}$ at node i and time level n.

$\hat{h}'_i$ • Predicted head at node i during a conversion from confined to unconfined flow.

$\hat{\underline{h}}$ • Vector of entries $\hat{h}_i$; $\hat{\underline{h}}_n$ is a vector of entries $\hat{h}_{i,n}$.

$\bar{\underline{h}}$ • Weighted mean of $\hat{\underline{h}}$ over time element n+1; defined by equation (63).

$\hat{\underline{h}}^*$ • Predicted head vector for time level n+1 for predictor-corrector method.

$\underline{h}_o$ • Arbitrary initial head vector for steady-state flow problems.

$I(\hat{e})$ • Error functional defined by equation (15) for Cartesian coordinates and by equation (214) for axisymmetric cylindrical coordinates.

$I_{mi,n}$ • The mth term of the infinite series for transient leakage at time level n resulting from time variation of head in the aquifer at node i; defined by equation (172).

$\hat{I}_{mi,n}$ • The mth term of the finite series to approximate transient leakage at time level n resulting from time variation of head in the aquifer at node i; defined by equation (179).

- $(\tilde{i},\tilde{j})$ • Row and column location of nonzero entries in $\underline{\underline{A}}$.
- $J_{mi,n}$ • The mth term of the infinite series for transient leakage at time level n resulting from time variation of head at the distal side of a confining unit at node i; defined by equation (175).
- $\hat{J}_{mi,n}$ • The mth term of the finite series to approximate transient leakage at time level n resulting from time variation of head at the distal side of the confining unit at node i; defined by equation (181).
- $\left(K_{xx}, K_{xy}, K_{yx}, K_{yy}\right)$ • Components of the hydraulic conductivity tensor for the aquifer written using Cartesian coordinates (x,y). Principal components in the $(\bar{x},\bar{y})$ coordinate system are $\left(K_{\bar{x}\bar{x}}, K_{\bar{y}\bar{y}}\right)$.
- $\left(K_{rr}, K_{zz}\right)$ • Principal components of the hydraulic conductivity tensor written using axisymmetric cylindrical coordinates (r,z).
- K'_{zz} • Vertical hydraulic conductivity in a confining unit; K'^{e}_{zz} is the constant value of K'_{zz} for spatial element e.
- $L_{ij'}$ • Length of the side of an element between nodes i and j'.
- $M_1\left(\Delta t_D\right)$ • Finite series approximation of $S_1\left(\Delta t_D\right)$ for transient leakage.
- $M_2\left(\Delta t_D\right)$ • Finite series approximation of $S_2\left(\Delta t_D\right)$ for transient leakage.
- $\underline{\underline{M}}$ • Preconditioning matrix that is an approximation of $\underline{\underline{A}}$ but is much easier to invert; defined by equation (266).
- N • Number of nodes in the finite-element mesh, or the number of unknowns in equation (254), depending on context.
- N_1, N_2 • Number of terms in $M_1\left(\Delta t_D\right)$ and $M_2\left(\Delta t_D\right)$, respectively.
- N_i^e • Basis functions for spatial finite elements defined by equation (9) for Cartesian coordinates and equation (211) for axisymmetric cylindrical coordinates. Overbar signifies evaluation using $(\bar{x},\bar{y})$ coordinates.
- $\underline{\underline{N}}$ • Matrix $\underline{\underline{A}}$-$\underline{\underline{M}}$.
- P • $\sum_{j=1}^{p} \delta\left(x-a'_j\right)\delta\left(y-b'_j\right)Q_j(t)$, which is the designation of p sources or sinks, each of strength Q_j, defined for equation (1).
- Q_j • Volumetric flow rate for point source or sink j; defined for equation (1).
- Q_{ai} • Volumetric flow rate at node i from leakage through a confining unit or river overlying an aquifer being dewatered.
- Q_{ei} • Volumetric flow rate at node i from areal head-dependent discharge.
- Q_{pi} • Volumetric flow rate at node i from point head-dependent discharge.
- Q_{ri} • Volumetric flow rate at node i from line head-dependent discharge.
- q_B • Specified flow (specific discharge times aquifer thickness) normal to a boundary.
- q_n • Normal component of flow (specific discharge times aquifer thickness) at a boundary.
- R • Hydraulic conductance of a confining unit; R^e is the constant value of R for spatial element e.
- (r,z) • Radial and vertical coordinates of the axisymmetric cylindrical coordinate system.
- $\underline{r}_\ell$ • Residual vector $\underline{B}_\ell - \underline{\underline{A}}_\ell \underline{\hat{h}}_\ell$ for the finite-element matrix equations at iteration ℓ.
- S • Storage coefficient of the aquifer; S^e is the constant value of S for spatial element e.

- S_s • Specific storage; S_s^e is the constant value of S_s for spatial element e.
- S_s' • Specific storage of a confining unit; $S_s'^e$ is the constant value of S_s' for spatial element e.
- S_y • Specific yield; S_y^e is the constant value of S_y for spatial element e.
- $S_1(\Delta t_D)$ • Infinite series for transient leakage; defined by equation (186).
- $S_2(\Delta t_D)$ • Infinite series for transient leakage; defined by equation (187).
- $\underline{s}_k$ • Displacement vector $\underline{x}_{k+1} - \underline{x}_k$ for the iterative GCGM method.
- $(T_{xx}, T_{xy}, T_{yx}, T_{yy})$ • Components of the transmissivity tensor for the aquifer written using Cartesian coordinates (x,y). Principal components in the $(\bar{x},\bar{y})$ coordinate system are $(T_{\bar{x}\bar{x}}, T_{\bar{y}\bar{y}})$.
- t • Time.
- t' • Time since time-level n, $t - t_n$.
- $\underline{\underline{U}}$ • Upper triangular matrix for symmetric-Doolittle factorization of $\underline{\underline{A}}$; defined by equation (259). Entries are u_{ij}, $i < j$, and α_{ii}.
- $\tilde{\underline{\underline{U}}}$ • Upper triangular matrix for incomplete-Cholesky or modified incomplete-Cholesky factorization of $\underline{\underline{A}}$; defined by equation (272). Nonzero entries are $\tilde{u}_{ij}$, $i < j$, and $\tilde{\alpha}_{ii}$.
- $\underline{\underline{V}}$ • Diagonal matrix defined by entries $V_{ii} = \sum_{e_i} v_{ii}^e$.
- v_B • Specified specific discharge normal to a boundary.
- v_n • Normal component of specific discharge at a boundary.
- v_{ii}^e • Hydraulic conductance and Cauchy-type boundary condition term defined by equation (37) for Cartesian coordinates and by equation (225) for axisymmetric cylindrical coordinates.
- W • Unit areal recharge or discharge rate for the aquifer; W^e is the value of W for spatial element e.
- (x,y) • Global Cartesian coordinates.
- $(\bar{x},\bar{y})$ • Local, rotated Cartesian coordinates along the principal directions of the transmissivity tensor.
- $\underline{x}$ • Solution vector for the finite-element matrix equation (254).
- $\underline{y}$ • Intermediate vector for the symmetric-Doolittle factorization solution of equation (254) or equation (269).
- z • Vertical coordinate direction, positive upward.
- z_b • Elevation of the aquifer base; z_{bi} is z_b at node i.
- z_e • Elevation below which the areal head-dependent discharge function vanishes; z_{ei} is z_e at node i.
- z_p • Elevation below which the point head-dependent discharge function vanishes; z_{pi} is z_p at node i.
- z_r • Elevation at which discharge to the aquifer from a line head-dependent source or sink is at a maximum; z_{ri} is z_r at node i.
- z_t • Elevation of the top of the aquifer (base of the confining unit); z_{ti} is z_t at node i.

Greek

- α • Parameter for Cauchy-type boundary conditions in Cartesian coordinates; defined by equation (4).
- α' • Parameter for Cauchy-type boundary conditions in axisymmetric cylindrical coordinates; defined by equation (209).
- α_{ii} • Entry of matrix $\underline{\underline{D}}^{-1}$.
- $\tilde{\alpha}_{ii}$ • Entry of matrix $\underline{\underline{\tilde{D}}}^{-1}$.
- α_m, β_m • Exponents defined by equations (176) and (177) used to approximate the infinite series for transient leakage calculations.
- γ_i • Transient leakage parameter for node i; defined by equation (167).
- Δ^e • Area of element e; defined by equation (11) for Cartesian coordinates and by equation (213) for axisymmetric cylindrical coordinates.
- Δt_n • Time interval $t_n - t_{n-1}$ for time element n.
- Δt_D • Dimensionless time interval $\gamma_i \Delta t_n$.
- $\underline{\delta}$ • Head change vector $\frac{2}{3}\left(\hat{\underline{h}}_{n+1} - \hat{\underline{h}}_n\right)$ over time interval $\frac{2}{3}\Delta t_{n+1}$ for unsteady-state problems; $\underline{\delta}_\ell$ is head change $\hat{\underline{h}}_{\ell+1} - \hat{\underline{h}}_\ell$ from iteration ℓ to iteration $\ell+1$ for nonlinear, steady-state problems.
- $\underline{\delta}^*$ • Predicted head change vector over time interval $\frac{2}{3}\Delta t_{n+1}$ for predictor step of the predictor-corrector method.
- $\underline{\delta}_o$ • Head change vector $\hat{\underline{h}} - \underline{h}_o$ computed for linear steady-state problems.
- ϵ • Convergence criterion for the MICCG method; defined for equation (285).
- ϵ_s • Convergence criterion for the iterative solution of nonlinear steady-state flow problems; defined for equation (240).
- θ^e • Counter-clockwise rotation angle from (x,y) coordinates to $(\bar{x},\bar{y})$ coordinates in element e.
- θ_i • Proportionate point in time element n+1 when node i converts from confined to unconfined flow or vice versa.
- $\hat{\theta}_i$ • The estimate of θ_i given by equation (96).
- σ_n, σ_{n+1} • Basis functions for time elements; defined by equation (13).
- ϕ_i • Proportionate point in time element n+1 when a point head-dependent discharge function, an areal head-dependent leakage function, or line head-dependent leakage function changes form at node i.
- ϕ'_i • $\phi_i\left(\phi_i + 1\right)/2$.
- ϕ_{ei} • Proportionate point in time element n+1 when an areal head-dependent discharge function changes form at node i; defined by equation (134).
- ϕ'_{ei} • $\phi_{ei}\left(\phi_{ei} + 1\right)/2$.
- ϕ_{ti} • Proportionate point in time element n+1 when an areal head-dependent discharge function changes form at node i; defined by equation (133).
- ϕ'_{ti} • $\phi_{ti}\left(\phi_{ti} + 1\right)/2$.